Nuclear Dynamics in Resonant Electron Collisions with Small Polyatomic Molecules

***T. N. Rescigno*[1], C. W. McCurdy[1,2], D. J. Haxton[3], C. S. Trevisan[2] and A. E. Orel[2]**

[1]Lawrence Berkeley National Laboratory, Berkeley, CA 94720, USA
[2]University of California, Davis, CA 95616, USA
[3]Universitry of Colorado and JILA, Boulder, CO 80309, USA

E-mail: tnrescigno@lbl.gov

Abstract. The excitation and dissociation of polyatomic molecules by low-energy electron impact can be dominated by resonant collision processes. The formal resonance theory that has formed the basis for much of our understanding of these processes has, for the most part, treated the nuclear dynamics in one dimension. This talk will focus on dramatic effects in low energy electron scattering by small molecules that are purely polyatomic in origin and that can only be studied with a multi-dimensional treatment of the dissociation dynamics. Resonant vibrational excitation of CO_2 and dissociative electron attachment to formic acid are briefly described to illustrate the discussion. The talk will then concentrate on the recent progress that has been made in studying dissociative electron attachment to water, including a completely ab initio evaluation of the three complex-valued resonance potential surfaces involved as well as the dynamical studies, carried out in full dimensionality, that give the state-specific cross sections and branching ratios into various two- and three-body channels.

1. Introduction

Resonant collisions of electrons with molecules are one of the most efficient pathways for the transfer of energy from electronic to nuclear motion. The formal resonance theory [1] that has been used to describe such collisions was developed over forty years ago. While this theory has been refined over the years with sophisticated and elaborate non-local treatments of the reaction dynamics [2], such studies have for the most part treated the nuclear dynamics in one dimension. This situation has resulted from the fact that, as the field of electron-molecule scattering developed, both experimentally and theoretically, the phenomena of vibrational excitation and dissociative attachment were first understood for diatomics, and it seemed natural to extend that understanding to polyatomic molecules using one-dimensional or single-mode models of the nuclear motion. However a series of experimental measurements of these phenomena in small polyatomic molecules have proven to be uninterpretable in terms of atomic motion with a single degree of freedom. Why do resonant collisions of electrons with CO_2 preferentially excite particular members of nearly degenerate groups (Fermi polyads) of vibrational levels [3, 4]? How does a π shape resonance in electron scattering from formic acid produce dissociative attachment products of an obviously different symmetry? Why does dissociative attachment of electrons to H_2O at 6.5 eV produce primarily H^- + OH while attachment at 11.5 eV produces mostly O^- + H_2? The answers to these questions involve multidimensional nuclear motion, multiple potential

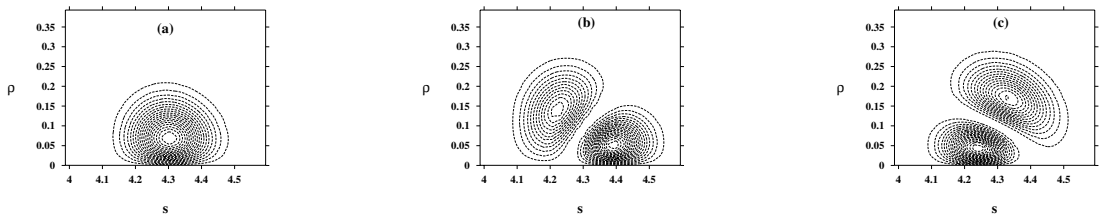

Figure 1. CO_2 vibrational wave functions calculated on the SCF surface (times bending normal coordinate $\rho^{1/2}$). (a) ground state, (b) lower member of Fermi dyad, (c) upper member of dyad. The normal coordinates ρ and s are in atomic units.

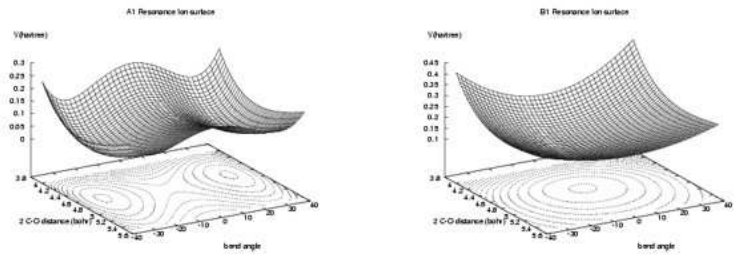

Figure 2. Real parts of the two components of the $^2\Pi_u$ CO_2^- resonance surface. Left:$^2A_1$; right: $^2B_1$

surfaces for the metastable anions, and conical intersections [5, 6, 7]. Using *ab initio* methods of electron scattering and bound state quantum chemistry we can generate those multidimensional potential surfaces for small molecules. With wave packet propagation on those coupled surfaces we can elucidate the mechanisms and reveal how they are probed in the experiments. It appears that these complexities are a general feature of electronic collisions with polyatomic molecules, and that they may hold the key to understanding how collisions of low-energy electrons produced by ionizing radiation damage biological molecules.

2. Two illustrative examples

Before turning to the subject that will form the major part of this talk, we will motivate the discussion with two examples that illustrate how polyatomic effects can play a key role in resonant electron collision processes. The first example is that of CO_2, which is a problem we looked at several years ago [8, 9]. Resonant vibrational excitation of CO_2 by electrons via the 3.8 eV $^2\Pi_u$ shape resonance offers a perfect example of nuclear excitation dynamics that are instrinsically polyatomic in origin. In CO_2, the near degeneracy of the zeroth-order symmetric stretch and bending levels ($\nu_{stretch} \approx 2\nu_{bend}$), or "Fermi resonance" phenomenon, leads to a complete breakdown of the single-mode description of the excited vibrational states [8]. One must therefore employ, at minimum, a two-dimensional treatment of the nuclear dynamics just to describe the relevant excited vibrational states (see Fig. 1). The other key fact is that the 3.8 eV shape resonance, of $^2\Pi_u$ symmetry in linear geometry, splits into two non-degenerate resonance states ($^2A_1$ and $^2B_2$) upon bending, which are coupled by Renner-Teller forces [9]. Moreover, the behavior of both the resonance energies and lifetimes for these states is markedly

different as the bending coordinate increases (see Fig. 2). The lower $^2A_1$ resonance surface decreases rapidly in energy, with a corresponding increase in the width, as one moves away from linear geometry. Without consideration of the $^2B_2$ state, one would find a broad, structureless peak in the vibrational excitation cross section. The $^2B_2$ state, however, increases in energy with a more or less constant width away from linear geometry. Since the two states are coupled, a portion of the initial wavepacket placed on the resonance surface(s) is trapped on the $^2B_2$ surface, which then feeds the lower surface and leads to "boomerang" structure in the observed cross sections (see Fig. 3). Since the overlaps of the decaying wavepacket onto the two quasi-degenerate components of the Fermi dyad are markedly different, the resulting cross sections show a different dependence on electron impact energy. None of this can be explained with a one-dimensional treatment.

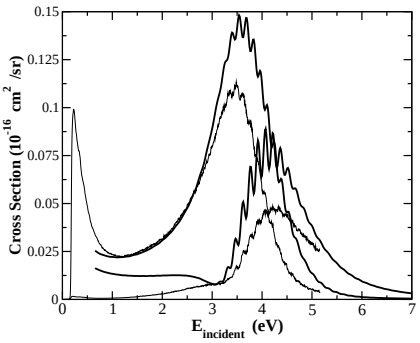

Figure 3. Differential vibrational excitation cross sections at 135° for upper and lower members of the Fermi dyad in CO_2. Thick solid curves were calculated and thin solid curves are experimental results of Allan([3]).

A second example of intrinsically polyatomic nuclear dynamics is afforded by low energy dissociative electron attachment by formic acid, HCOOH. Experiment [10] shows a strong peak in the DEA spectrum near 1.3 eV incident electron energy, with a width of ∼0.5 eV, which correlates with production of formate ($HCOO^-$) anions. The experimental observation is that DEA proceeds with an almost vertical onset that is close to the thermodynamic threshold for the process and also gives some indication of fine structure oscillations on the high-energy tail of the peak.

Fixed-nuclei calculations carried out at the equilibrium target [11] geometry show a low-energy π^* shape resonance that falls within the appropriate energy range, typical of those found in other small unsaturated molecules such as N_2, CO, CO_2, H_2CO, C_2H_4 and C_2F_4. The energies and lifetimes of such resonances are usually sensitive to small changes in the length of the unstaurated bond. It may be logical to assume that this resonance is in some way involved in the observed DEA channel, but there are several complicating factors. One obvious problem is that it is the OH bond that must be broken in forming the formate anion (see Fig. 4) and not the carbonyl bond which initially traps the electron. Moreover, there are symmetry issues that argue against a simple interpretation of the experimental results. At its equilibrium geometry, formic acid is a planar molecule, belonging to the point group C_s. In planar geometry, its neutral and anion states can be classified either as A′ or A″, the latter being antisymmetric under reflection through the molecular plane. The formate anion also has a closed-shell, planar (A′) structure, and ground-state atomic hydrogen is A′, since it is, of course, ^2S. Capture of an electron into a π^* resonance orbital produces a negative ion state of A″ symmetry. Therefore, in order to produce A′ fragments, the planar symmetry must be broken along the reaction path, allowing interaction with a second anion state that can dissociate to the observed fragments. The reaction occurs because of the coupling of the mulitple degrees of freedom in this system, which is an inherently polyatomic effect.

A series of fixed-nuclei calculations show that the reaction path for the π^* resonance involves an initial increase in the C=O and C-O bond distances, followed by a symmetry-breaking

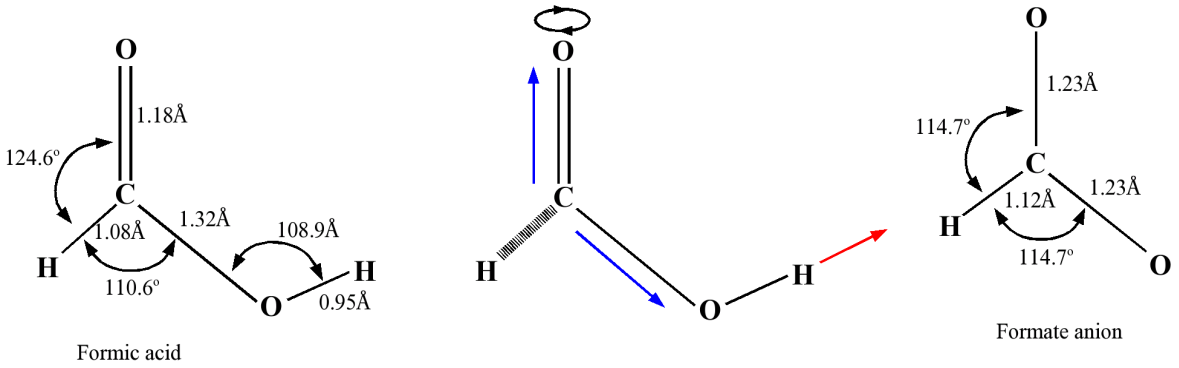

Figure 4. Equilibrium geometries of formic acid and formate anion, as well as negative ion intermediate. Angles are in degrees and distances are in units of angstroms.

distortion in which the hydrogen which is bonded to carbon is moved out of the plane of the other nuclei. As the OH bond distance is increased in the non-planar geometry, the π^* resonance surface is found to have a conical intersection with a second ^{2}A' anion state, which does correlate with $HCOO^-$+H with increasing OH distance. Thus, DEA to the experimentally observed fragments appears to follow an adiabatic path on which the π^* state changes character and becomes the $2A'$ anion state. No simple one-dimensional treatment of the nuclear dynamics can explain such phenomena.

3. Dissociative electron attachment to water

The dissociative attachment of electrons to gas-phase water molecules is governed by complex nuclear and electronic dynamics. Three resonance peaks have been identified, which have been associated with anion states of $^2B_1$, $^2A_1$ and $^2B_2$ symmetry, with cross section maxima near incident electron energies of 6.4, 8.4, and 11.2 eV. The dominant anion produced is H^-, which comes principally from the lowest energy ($^2B_1$) channel, with a peak cross section of $\sim 6.5 \times 10^{-18}$cm^2. The $^2A_1$ resonance also produces H^-, with a peak cross section down by a factor of five, while the third ($^2B_2$) resonance produces no H^-. O^- represents the minor channel, with a peak cross section roughly ten times smaller that the H^- cross section, and comes mainly from the $^2B_2$ state, with smaller (by a factor of two) amounts from the $^2A_1$ resonance and even less from the lowest, $^2B_1$, resonance. Curiously, the energetically favored OH^-, seen in some early experiments, is not believed to be a direct product of low-energy dissociative electron attachment to water, but may come instead from water clusters [12]. In the recent work of Fedor *et al.* [13], it is argued that small amounts of OH^- are seen as a direct product of DEA to water, but no mechanism has yet been advanced to explain this minor channel.

To understand the basics of DEA to water [14, 15], it is useful to recall that, *near equilibrium geometry* ($r_1 = 1.81$ bohr, $r_2 = 1.81$ bohr, $\theta = 104.5°$), the ground state of H_2O is well described by a self-consistent field (SCF) wave function with orbitals, in order of increasing energy, labeled $\{1a_1, 2a_1, 1b_2, 3a_1, 1b_1\}$ in C_{2v} symmetry or $\{1a', 2a', 3a', 4a', 1a''\}$ in C_s symmetry. There are six low-lying dissociative electronic states of water -$^{1,3}B_1$, $^{1,3}A_1$, and $^{1,3}B_2$ - which, near equilibrium geometry, are well described by promoting an occupied $1b_1, 3a_1$, or $1b_2$ electron into the anti-bonding $4a_1$(5a") orbital. These states are the parents of three doubly excited (Feshbach) anion states with configurations $1b_1 4a_1^2$, $3a_1 4a_1^2$, and $1b_2 4a_1^2$, corresponding to the three main dissociative attachment peaks. In addition, there are also $^{3,1}A_2$ excited states in this energy range, of predominantly Rydberg character, obtained by promoting a $1b_1$ electron into the unoccupied $2b_2$ orbital.

We undertook an extensive study of DEA to water with a view toward treating, from first principles, all aspects of an electron polyatomic collision, including not only the determination of the fixed-nuclei electronic cross sections, but also a treatment of the nuclear dynamics in full dimensionality [14, 15, 16, 17, 18]. Such a treatment first entails constructing complete surfaces for the relevant anion states. A resonance state may be characterized by a width, Γ, and an energy, E_R, which are functions of the internuclear geometry $\vec{q}$. These quantities define a complex potential surface $V(\vec{q})$,

$$V(\vec{q}) = E_R(\vec{q}) - i\frac{\Gamma(\vec{q})}{2}. \tag{1}$$

The width Γ is related to the lifetime as $\tau = 1/\Gamma$. For a triatomic, the internal coordinates $\vec{q}$ may be the set of bond-angle coordinates (r_1, r_2, θ). We used different techniques to define the two components of the potential energy surfaces, $E_R(\vec{q})$ and $\Gamma(\vec{q})$. To compute $\Gamma(\vec{q})$, we performed fixed-nuclei scattering calculations using the complex Kohn variational method [19] and extracted the resonance positions and widths from the energy dependent $T-$matrices.

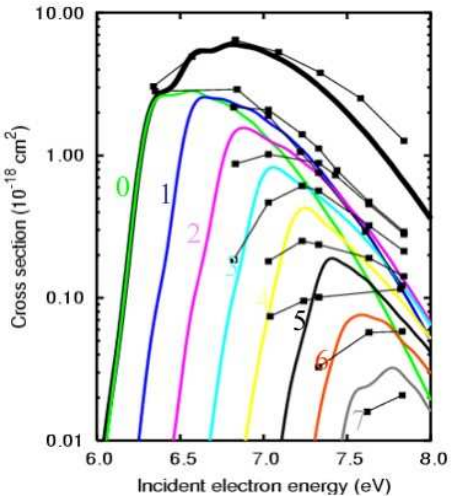

Figure 5. Cross sections for (000) initial state, total (heavy line) and into vibrational channels $\nu = 0$ through $\nu = 7$ of OH (dotted lines, left to right), on a logarithmic scale. Also included are data from Belič, Landau and Hall's[20] measurements (thin lines with squares), shifted in energy so that the maxima (present, 6.81eV, versus their value of 6.5eV) in the total cross section coincide.

Although the electronic scattering calculations yield both energy positions and widths, the values of E_R we used came from more elaborate configuration-interaction (CI) calculations. In the asymptotic regions, where the resonances become electronically bound states, the use of bound-state methods is entirely appropriate. Near the Franck-Condon region where these states are resonances, our CI treatment restricted the included configuration space to eliminate the ground state electronic continuum from the calculation. Thus our CI calculations neglect the shift in E_R due to coupling with that continuum, a well-known effect explained by the Feshbach resonance formalism [21]. Since the shift in E_R by this coupling is generally of the same order as the width, Γ, this is an excellent approximation in regions where the resonances are narrow. In the Franck-Condon region, the three Feshbach resonance states of interest have as their dominant configuration an electron attached to a singly excited configuration of the neutral target and thus tend to have small widths. Once the complex resonances surfaces are computed and fitted, the nuclear dynamics problem was solved using the local complex potential model. To apply the local complex potential model to a polyatomic system, we make use of a time-dependent formulation that simplifies both the numerical calculations and the physical interpretation of the dynamics. We used the Multiconfiguration Time Dependent Hartree (MCTDH) method [22] to solve the working equations. This time-dependent approach, combined with the power of the MCTDH implementation, is the key to treating polyatomic dissociative attachment and resonant vibrational excitation problems.

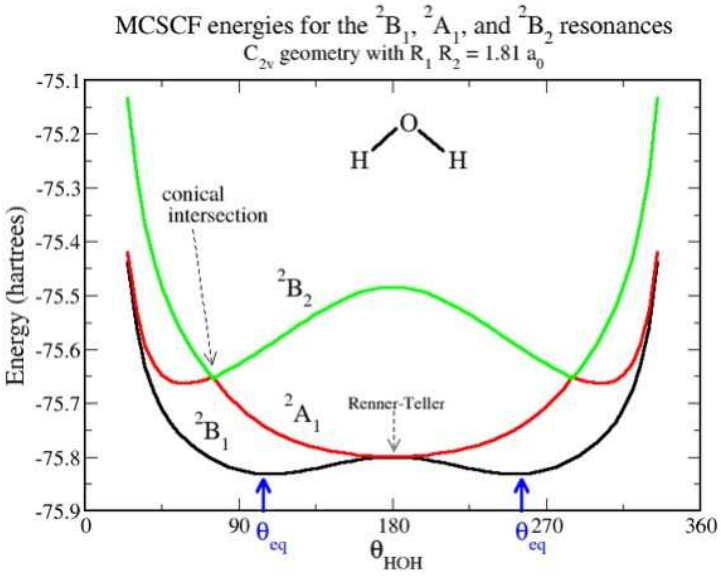

Figure 6. Real parts of resonance energies, in units of hartrees, for OH bond distance = 1.81 a_0 in C_{2v} geometry, plotted with respect to bending angle.

Figure 5 shows cross sections for the dominant channel, production of H^- via the $^2B_1$ resonance, for different OH product vibrational states. The calculations [15] are seen to be in good agreement with experiment. In the vicinity of the equilibrium geometry of the neutral ($r_1 = r_2 = 1.81$ bohr; $\theta = 104.5°$) the gradient of the real part of the resonance energy is steeply downhill in the r_1 or r_2 directions. Since the wavepacket begins high upon the repulsive wall of the resonant state, it acquires a large amount of momentum in the symmetric stretch direction, which becomes vibrational and translational motion in the H^- + OH wells. This dynamics is the origin of vibrational excitation in the product fragment, and it is one of the central qualitative results of this study of the dynamics of dissociative attachment through the $^2B_1$ resonance. In contrast to its dependence on r_1 or r_2, the $^2B_1$ potential is relatively flat in θ. The H_2 + O^- well can only be reached if the bond angle θ is decreased substantially from the equilibrium geometry of the neutral, whereas the OH + H^- channel is immediately adjacent to the initial wavepacket. Therefore, the wavepacket proceeds downhill towards the OH + H^- arrangement channel, with very little density arriving in the H_2 + O^- exit channel.

Turning to the question of O^- production, we are presented with something of a puzzle. O^- is produced principally from the $^2B_2$ resonance, yet this resonance surface does not have O^- as one of its asymptotes. The answer to the puzzle is that the $^2B_2$ surface has a conical intersection with the $^2A_1$, as depicted in Fig. 6 which shows the behavior of the resonance states as a function of HOH bond angle for a fixed bond distance in C_{2v} geometry. A wavepacket initiating on the $^2B_2$ surface near the target equilibrium bond angle will tend to move on an energetically downhill path toward the conical intersection. Non-adiabatic coupling can lead to a portion of the surviving wavepacket leaking onto the lower $^2A_1$ surface and ultimately finding its way to the O^- product channel. Figure 7 shows the results of our calculations [18] for DEA leading to O^- product. We do indeed find O^- coming from the highest resonance, but the magnitude of cross section is significantly lower than the recently reported measurements of Fedor *et al.* [13]. So having solved one puzzle, we are now confronted with another: why is the O^- cross section arising from the $^2B_2$ resonance so much smaller than the observed value and why do we find

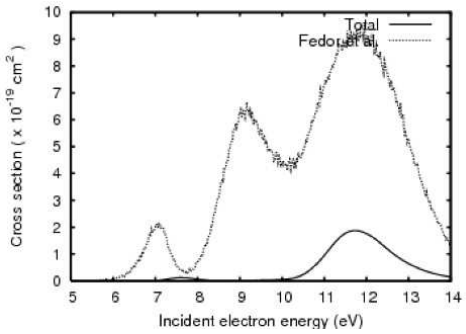

Figure 7. O^- production from dissociative electron attachment to water. Experimental results from ref. [13]

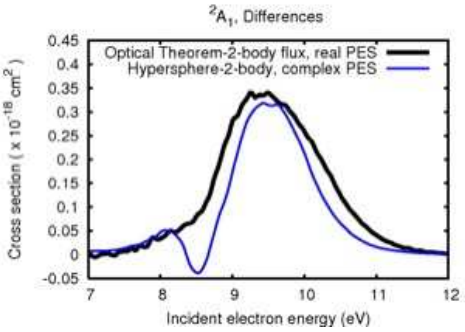

Figure 8. Comparison of cross sections for O^- production from $^2A_1$ via three-body breakup, computed from optical theorem and from hyperspherical outgoing flux.

virtually no O^- coming from the $^2A_1$ resonance when it is clearly observed experimentally?

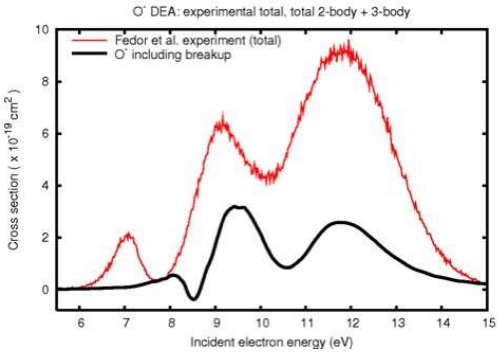

Figure 9. As in Fig. 7, with calculations including three-body contribution from $^2A_1$ resonance.

To answer these final questions we must turn to DEA leading to three-body breakup, i.e. to the product channel H+H+O^-, whose threshold is 8.04 eV. Our published studies of DEA [15, 18] have reported the results of calculations carried out in Jacobi coordinates and the cross sections were obtained by summing the results for DEA into the individual rovibrational states $\chi_{j\nu}$ for the appropriate ion + diatom arrangement. The complex absorbing potential flux formalism [22] which we employed within the MCTDH implementation [23] is not appropriate for the three-body breakup channel when used in conjunction with Jacobi coordinate systems. We have therefore carried out a new series of calculations to assess the importance of three-body breakup in connection with O^- production via the $^2A_1$ resonance. We first computed the total reaction cross section using the optical theorem. This test requires a real potential, so we dropped the imaginary portion of the resonance potential surface, thereby closing the vibrational excitation channels and restricting the total reaction probability to go into DEA channels. We also recomputed the sum of all two-body DEA cross sections using the same real potential.To estimate the three-body contribution to DEA, we simply substract the sum of the two-body cross sections from the total reactive cross section obtained from the optical theorem. We then carried out a second set of calculations, using the full complex potential surface, in hyperspherical coordinates, and computed the total cross section from the outgoing flux through a hypersphere placed in the asymptotic region. The three-body cross sections were again obtained by subtracting the sum of our originally computed two-body DEA cross sections from the total cross section. The results of these two treatments, plotted in Fig. 8, are seen to give very similar results. Figure

9 replots the cross sections for O^- production, including the three-body contribution from the $^2A_1$ state. Similar calculations are underway for O^- from $^2B_2$. At this point, we feel that any remaining discrepancies between our calculations and experiment can be attributed to errors in our calculated resonance surfaces, but that our theoretical treatment has captured the essential physics of the problem.

4. Conclusions

We have tried to demonstrate that, even in the case of relatively simple polyatomic molecules, both vibrational excitation and dissociative attachment can involve *intrinsically polyatomic dynamics*, not described by one-dimensional models. Multiple coupled resonance potential surfaces can be involved, e.g. Renner-Teller coupling in the case of CO_2^- and conical intersections in the case of formic acid and water anions. We have also seen that complete breakup into three-body channels can be an important mechanism for some channels in dissociative attachment, e.g., the O^- channel of dissociative attachment to water via both $^2A_1$ and $^2B_2$ resonances, even at energies close to threshold. Indeed, when looking at dissociative electron attachment in more complex systems, particularly in targets of biological relevance, it may well be the case that conical intersections between resonances may be the norm, not the exception. This raises an interesting challenge for future work in this area: there is currently no viable extension of nonlocal theories of resonance dynamics to polyatomic molecules. It is now well established that nonlocal effects are frequently necessary for the quantitative description of resonance processes in diatomics, so finding viable extensions of these theories to polyatomics will be very important.

Acknowledgments

This work was performed under the auspices of the US Department of Energy by the University of California Lawrence Berkeley National Laboratory under Contract DE-AC02-05CH11231 and was supported by the U.S. DOE Office of Basic Energy Sciences, Division of Chemical Sciences. CWM and AEO acknowledge support from the National Science Foundation.

References

[1] O'Malley T F 1966 *Phys. Rev.* **150** 14
[2] Domcke W 1991 *Phys. Rep.*. **208** 97
[3] Allan M 2000 *Phys. Rev. Lett.* **87** 033201
[4] Johnstone W M, Akther P and RNewell W 1995 *J.Phys. B* **28** 743
[5] Skalicky T, Chollet C, Pasquier N and Allan M 2002 *Phys. Chem. Chem. Phys.* **4** 3583
[6] Anusiewicz I, Sobczyk M, Berdys-Kochansks J, Skurski P and Simons J 2005 *J. Phys. Chem.* **109** 484
[7] Scheer A M, Aflatooni K, Gallup G A and Burrow P D 2004 *Phys. Rev. Lett.* **92** 068102
[8] Rescigno T N, Isaacs W A, Orel A E, Meyer H D and McCurdy C W 2002 *Phys. Rev. A* **65** 032716
[9] McCurdy C W, Isaacs W A, Meyer H D and Rescigno T N 2003 *Phys. Rev. A* **67** 042708
[10] Pelc A, Sailer W, Scheier P, Mason N J and Märk T D 2002 *Eur. Phys. J. D* **20** 441
[11] Rescigno T N, Trevisan C S and Orel A E 2006 *Phys. Rev. Lett.* **96** 213201
[12] Klots C E and Compton R N 1978 *J. Chem. Phys.* **69** 1644
[13] Fedor J, Cicman P, Coupier B, Feil S, Winkler M, Gluch K, Husarik J, Jaksch D, Farizon B, Mason N J, Scheier P and Märk T D 2006 *J. Phys B* **39** 3935
[14] Haxton D J, Zhang Z, McCurdy C W and Rescigno T N 2003 *Phys. Rev. A* **69** 062713
[15] Haxton D J, Zhang Z, Meyer H D, Rescigno T N and McCurdy C W 2003 *Phys. Rev. A* **69** 062714
[16] Haxton D J, Rescigno T N and McCurdy C W 2005 *Phys. Rev. A* **72** 022705
[17] Haxton D J, McCurdy C W and Rescigno T N 2007 *Phys. Rev. A* **75** 012710
[18] Haxton D J, Rescigno T N and McCurdy C W 2007 *Phys. Rev. A* **75** 012711
[19] Rescigno T N, Lengsfield B H and McCurdy C W 1995 *Modern Electronic Structure Theory* vol 1 ed Yarkony D R (Singapore: World Scientific) p 501
[20] Belič D S, Landau M and Hall R I 1981 *J. Phys. B.* **14** 175–190
[21] Feshbach H 1962 *Ann. Phys.* **19** 287
[22] Beck M, Jäckle A, Worth G and Meyer H D 2000 *Phys. Reports* **324** 1–105

[23] Worth G, Beck M, Jäckle A and Meyer H D 2000, The MCTDH Package, Version 8.2 (2000). Meyer H D, Version 8.3 (2002). See http://www.pci.uni-heidelberg.de/tc/usr/mctdh/.